

Solving the Source Localization Problem via Global Distance Continuation

Giuseppe Destino and Giuseppe Thadeu Freitas de Abreu
 Center for Wireless Communications
 University of Oulu, Finland
 E-mails: [destino, giuseppe]@ee.oulu.fi

Abstract—A new optimization algorithm is presented for the solution of the range-based source-localization problem employing a least-squares (LS) multidimensional scaling (MDS) formulation over *non-squared* distances. The algorithm is based on an progressive objective-smoothing technique known as global distance continuation (GDC). The fundamental requirements to implement a GCD method, namely, expressions for the smoothed cost-function and its derivatives, and lower bound on the starting value of the smoothing parameter λ , are all derived analytically. The GDC method is known to be stable, fast and insensitive to initial point. Since distance measurement errors are a major cause of degradation in localization systems, by providing a GDC algorithm that does not require squaring measured distances we add to the latter advantages further robustness to noise. The performance of the resulting linear-distance GDC algorithm is evaluated via extensive Monte Carlo analysis and comparisons to a) the conventional squared-distance GDC algorithm, b) a Newton-based optimization technique of similar complexity, and c) the (impractical) grid-based exhaustive search method, *i.e.*, maximum-likelihood (ML) estimator. The results reveal that the linear-distance GDC algorithm outperforms the considered alternatives and achieves the performance of the ML estimator.

I. INTRODUCTION

Location-awareness is considered as a pivotal feature of novel wireless communication systems. In cellular systems, for instance, several applications and services recently introduced¹ or under development rely on the assumption that information about the location of wireless terminals is available to the network, and indoor networks dedicated to or featuring positioning applications are been designed [1].

The recent developments motivate research aimed at improving the accuracy of localization algorithms formulated for a number of different scenarios. In this article we will focus on a “single-target” formulation where, the network is modeled by a single device of unknown location (target) and a few nodes with fixed and known locations (anchors), all of which are interconnected. This scenario describes, for instance, the case of a cellular location-based services (LBS).

In this case, the localization problem consists of estimating the position of the target from a set of measurements of its distance to the anchors. In the literature, this is known as the range-based source-localization problem, although the actual localization algorithm can also run on the target (self-localization).

Mathematically, the source-localization and self-localization problems are equivalent, and the metric least-squares (LS) multidimensional scaling (MDS) [2] is the framework of choice to formulate them. The major difficulty thereby is the minimization of the LS-MDS cost-function (objective), which is known to be non-convex. This is critical because non-convex optimization methods are either too complex or too sensitive to initialization points, both of which are undesired, especially in the self-localization case where battery power is limited and a smooth and prompt localization experience is valued.

Semidefinite programming (SDP) [3], [4] and simulated annealing (SA) [5], for instance, are effective non-convex optimization techniques, but their complexities orders are geometrically proportional to the number of nodes² in the network – $\mathcal{O}(N^6)$ and $\mathcal{O}(N^4)$, respectively. In contrast, stress-majorization (SMACOF) [2], [6] and Newton-based approaches [7] are much simpler, but may yield poor results if the initialization point is not sufficiently accurate, as these techniques are more prone to convergence to local minima.

A less-known non-convex optimization algorithm that provides low computational complexity, robustness to the local minima problem and very good accuracy is the global distance continuation (GDC) approach, proposed in [8]. The only deficiency of the GDC method, as proposed thereby, is the fact that it is based on a LS-MDS formulation of the localization problem that requires measured distances to be squared, which has been recently shown to be sub-optimal [9] to the LS-MDS formulation with basis on non-squared distance estimates. In this paper, a GDC-based minimization algorithm tailored to the optimal (linear-distance) LS-MDS approach [9] is proposed.

The GDC algorithm is a progressive objective-smoothing technique and requires expressions for the smoothed objective and its derivatives, as well as a lower bound on the starting value of the smoothing parameter. All such required functions are derived analytically here. The proposed algorithm is shown to outperform alternative low-complexity techniques and, in fact, to yield the same performance achieved with a fine grid-based exhaustive search method, which in optimization theory is the equivalent of the maximum-likelihood (ML) estimator.

The remainder of the paper is as follows. The source-localization problem and the GDC-based technique are formulated in Section II. The details of the GDC mechanism and its performance are given in sections III and IV, respectively.

¹Google Mobile Maps, South African Vodacom’s “The Grid” spatial-networking and the US’s E911 (FCC docket 94-102) are a few examples.

²While 3 anchors are sufficient to allow 2-dimensional localization, it is well-known that localization accuracy increases with N .

II. PROBLEM FORMULATION

A. Squared versus Non-squared Distances

Consider a simple cellular-based wireless network of N nodes deployed in the η -dimensional space. Assume that N_A nodes are base-stations (anchors) and only one node is the mobile terminal (target). The anchors' locations are known *a priori*, while the position of the target is yet to be determined.

Let $\mathbf{a}_i \in \mathbb{R}^\eta$ and $\mathbf{x} \in \mathbb{R}^\eta$ be row-vectors, whose elements indicate the Euclidean coordinates of the i -th anchor's and target's location, respectively. Let $d_i = \|\mathbf{a}_i - \mathbf{x}\|_2$ be the Euclidean distance between the i -th anchor and the target, where $\|\cdot\|_2$ is the Euclidean norm. A measurement of the distance d_i is denoted by \tilde{d}_i , which is generated accordingly with the ranging error model proposed in [10]–[12]:

$$\tilde{d}_i = d_i + n_i, \quad (1)$$

where n_i denotes the noise.

Under a weighted LS-MDS formulation, the source-localization problem consists of finding an estimate $\hat{\mathbf{x}}$ for the target's location that minimizes the weighted sum of the least-square error $\epsilon_i \triangleq (\tilde{d}_i^q - \hat{d}_i^q)$, thus

$$\hat{\mathbf{x}} = \arg \min_{\mathbf{x} \in \mathbb{R}^\eta} \sum_{i=1}^{N_A} w_i \left(\tilde{d}_i^q - \hat{d}_i^q \right)^2, \quad (2)$$

where q is an exponent selected amongst the values $\{1, 2\}$, $\hat{d}_i \triangleq \|\mathbf{a}_i - \hat{\mathbf{x}}\|_2$ and w_i is a weighing factor related to the concern [13] over the term ϵ_i .

Hereafter, equation (2) with $q=1$ and $q=2$ will be referred to as the *range*-based LS (R-LS) and *squared range*-based LS (SR-LS) source-localization problems, respectively.

It is well-known that the objective function in equation (2), denoted by $s(\hat{\mathbf{x}})$, is not convex, and that the number of its local-minima depends on both the geometry of the network and the amount of error affecting the distance measurements \tilde{d}_i 's [13], [14]. Furthermore, it has been shown [9] that the SR-LS based formulation ($q=2$) is sub-optimal to the R-LS formulation ($q=1$) in a maximum-likelihood (ML) sense. While an algorithm that yields an exact solution of equation (2) with $q=2$ was provided in [9], the case with $q=1$ is still an open problem. In the sequel, we proposed a GDC algorithm to solve equation (2) with $q=1$.

B. Formulation of GCD-based R-LS Localization Problem

The GDC-based optimization technique consists of an iterative procedure in which, at each k -th iteration, the original objective is smoothed by a kernel (smoothing function) prior to its minimization. The kernel is parameterized by a smoothing parameter λ , adjusted at each iteration, such that the sequence of successive $\lambda^{(k)}$ is strictly monotonically decreasing to zero ($\lambda^{(K)} = 0$) and, at $\lambda^{(1)}$, the smoothed objective is convex.

Consider the Gaussian kernel [8]

$$g(u, \lambda) \triangleq e^{-u^2/\lambda^2}. \quad (3)$$

Let $\langle s \rangle_\lambda(\hat{\mathbf{x}})$ denote the smoothed objective, given by

$$\langle s \rangle_\lambda(\hat{\mathbf{x}}) \triangleq \frac{1}{\pi^{\eta/2} \lambda^\eta} \int_{\mathbb{R}^\eta} s(\mathbf{u}) e^{-\frac{\|\mathbf{u} - \hat{\mathbf{x}}\|_2^2}{\lambda^2}} d\mathbf{u}, \quad (4)$$

where $s(\mathbf{u})$ is the objective function in equation (2), $\mathbf{u} \in \mathbb{R}^\eta$ and $\lambda \in \mathbb{R}^+$ is a parameter that controls the degree of smoothing ($\lambda \gg 0$ strong smoothing).

Using equation (2) with $q=1$, $\langle s \rangle_\lambda(\hat{\mathbf{x}})$ becomes

$$\langle s \rangle_\lambda(\hat{\mathbf{x}}) = \frac{1}{\pi^\eta} \int_{\mathbb{R}^\eta} \sum_{i=1}^{N_A} w_i \left(\tilde{d}_i - \|\mathbf{a}_i - \hat{\mathbf{x}} + \lambda \mathbf{u}\|_2 \right)^2 e^{-\|\mathbf{u}\|_2^2} d\mathbf{u}. \quad (5)$$

From all the above, the GDC-based R-LS formulation of the source-localization problem can be summarized as

$$\hat{\mathbf{x}}^{(K)} = \arg \min_{\substack{\mathbf{x} \in \mathbb{R}^\eta \\ k=1, \dots, K}} \langle s \rangle_{\lambda^{(k)}}(\hat{\mathbf{x}}). \quad (6)$$

The low-complexity of the algorithm results from two facts.

First, the total number of iterations K are fixed a priori and they can be kept small. Second, the effect of smoothing the original objective is to reduce the number of local minima, such that with an adequate amount of smoothing a low-complexity technique such as the steepest-descent [15] $\mathcal{O}(N^3)$ can be used to perform the minimization at the k -th iteration without compromising the effectiveness of the algorithm.

An efficient implementation of a GDC-based optimization requires closed-forms for the smoothed function and its derivative. In the sequel, the aforementioned requirements are derived analytically.

III. LINEAR-DISTANCE GDC ALGORITHM

In what follows, the fundamental expressions required to solve the GDC-based source localization problem as in equation (6) are derived.

A. Evaluation of $\langle s \rangle_\lambda(\hat{\mathbf{x}})$

It is shown in the appendix that with $\eta=2$, equation (5) reduces to

$$\langle s \rangle_\lambda(\hat{\mathbf{x}}) = \sum_{i=1}^{N_A} w_i \left(\lambda^2 - 2\lambda \tilde{d}_i \Gamma\left(\frac{3}{2}\right) {}_1F_1\left(\frac{3}{2}; 1; \frac{\tilde{d}_i^2}{\lambda^2}\right) e^{-\frac{\tilde{d}_i^2}{\lambda^2} + \tilde{d}_i^2 + \tilde{d}_i^2} \right), \quad (7)$$

where $\Gamma(a)$ is the gamma function and ${}_1F_1(a; b; c)$ is the confluent hypergeometric function [16].

The numeric evaluation of equation (7) requires care, especially when λ is very small. Numerically stable computations can be achieved using known equivalences for the confluent hypergeometric function [16]. In particular,

$${}_1F_1\left(\frac{3}{2}; 1; z\right) = 1 + \sum_{m=1}^{+\infty} \left(z^m \cdot \prod_{k=1}^m \frac{(1/2 + k)}{k^2} \right), \quad z < 10. \quad (8)$$

$${}_1F_1\left(\frac{3}{2}; 1; z\right) \approx \frac{z^{-3/2}}{\Gamma(-\frac{1}{2})} \left(\sum_{m=0}^{M-1} \frac{(-z)^{-m}}{m!} \prod_{k=0}^{m-1} \left(\frac{3}{2} + k\right)^2 \right) + \frac{e^z z^{1/2}}{\Gamma(\frac{3}{2})} \left(\sum_{q=0}^{Q-1} \frac{z^{-q}}{q!} \prod_{k=0}^{q-1} \left(k - \frac{1}{2}\right)^2 \right), \quad z \geq 10, \quad (9)$$

where $z \triangleq \frac{\tilde{d}_i^2}{\lambda^2}$ and M and Q are sufficiently large numbers to ensure an accurate approximation (typically $(M, Q) \geq 5$).

B. Derivatives of $\langle s \rangle_\lambda(\hat{\mathbf{x}})$

As mentioned above, the properties of the GDC method allows each k -th minimization of (6) to be performed with a simple steepest-descent algorithm, which for an efficient implementation requires the gradient $\nabla_{\hat{\mathbf{x}}} \langle s \rangle_\lambda(\hat{\mathbf{x}})$.

Start by noticing that $\langle s \rangle_\lambda$ is given by a non-negative weighted sum of a set of subfunctions s_i , defined as

$$s_i(\hat{d}_i; \lambda) \triangleq \tilde{d}_i^2 + \hat{d}_i^2 + \lambda^2 - \lambda \tilde{d}_i \sqrt{\pi} {}_1F_1\left(\frac{3}{2}, 1, \frac{\hat{d}_i^2}{\lambda^2}\right) e^{-\frac{\hat{d}_i^2}{\lambda^2}}, \quad (10)$$

where we used the fact that $\hat{d}_i = \|\hat{\mathbf{a}}_i - \hat{\mathbf{x}}\|_2$.

It will prove convenient in what follows to replace $r_i \triangleq \hat{d}_i$. Then,

$$\nabla_{\hat{\mathbf{x}}} \langle s \rangle_\lambda(\hat{\mathbf{x}}) = \sum_{e_i \in E} s'_i(r_i; \lambda) \nabla_{\hat{\mathbf{x}}} r_i \quad (11)$$

where the i -th $\eta \times \eta$ block $\nabla_{\hat{\mathbf{x}}} r_i$ is

$$[\nabla_{\hat{\mathbf{x}}} r_i]_i = \frac{\hat{\mathbf{a}}_i - \hat{\mathbf{x}}}{\|\hat{\mathbf{a}}_i - \hat{\mathbf{x}}\|_2}. \quad (12)$$

and s' is given by

$$s'(r; \lambda) = 2r + \frac{r\sqrt{\pi}\tilde{d}}{\lambda} S_1(r; \lambda), \quad (13)$$

where for notational simplicity we have (and will hereafter) omitted the subscript i and

$$S_1(r; \lambda) \triangleq e^{-\frac{r^2}{\lambda^2}} \left(2 {}_1F_1\left(\frac{3}{2}; 1; \frac{r^2}{\lambda^2}\right) - 3 {}_1F_1\left(\frac{5}{2}; 2; \frac{r^2}{\lambda^2}\right) \right). \quad (14)$$

For reasons to be clarified later, also the second derivative $s''(r; \lambda)$ is derived. Thus,

$$s''(r; \lambda) = 2 + \sqrt{\pi}\tilde{d} \left(\frac{1}{\lambda} - \frac{2r^2}{\lambda^3} \right) S_1(r; \lambda) + \frac{2\sqrt{\pi}\tilde{d}r^2}{\lambda^3} S_2(r; \lambda), \quad (15)$$

where

$$S_2(r; \lambda) \triangleq e^{-\frac{r^2}{\lambda^2}} \left(3 {}_1F_1\left(\frac{5}{2}; 2; \frac{r^2}{\lambda^2}\right) - \frac{15}{4} {}_1F_1\left(\frac{7}{2}; 3; \frac{r^2}{\lambda^2}\right) \right). \quad (16)$$

C. Computation of $\lambda^{(1)}$

The last critical step required to implement the above-described GDC algorithm is to determine the initial smoothing parameter $\lambda^{(1)}$, such that $\langle s \rangle_\lambda$ is convex, i.e., $\frac{d^2 s(r; \lambda)}{dr^2} > 0$, for all r . Using the fact that the positive sum of convex functions is also a convex function [13], and in view of equation (7), it follows that the convexity of $\langle s \rangle_\lambda$ is ensured by the convexity of all s_i 's. In order to establish the latter we will make use of the following Lemmas.

Lemma 1 (Properties of $S_1(r; \lambda)$):

- i) $S_1(0; \lambda) = -1$
- ii) $S'_1(r; \lambda) > 0$
- iii) $\lim_{r \rightarrow \infty} S_1(r; \lambda) = 0^-$

where 0^- indicates that the function approaches 0 from the negative side.

Proof: Property *i* is trivial, as ${}_1F_1(a; b; 0) = 1, \forall (a, b) > 0$.

In order to prove property *ii*, that is, the monotonicity of $S_1(r; \lambda)$, we make use of the recurrence relation [16, pp.508, 13.5.1]

$$(b-a) {}_1F_1(a; b+1; z) = b {}_1F_1(a; b; z) - b {}_1F'_1(a; b; z) \quad (17)$$

Hence,

$$\begin{aligned} S'_1(z; \lambda) &= \quad (18) \\ &= e^z \left(3 {}_1F_1\left(\frac{3}{2}; 1; z\right) - 2 {}_1F_1\left(\frac{5}{2}; 2; z\right) + 3 {}_1F_1\left(\frac{3}{2}; 1; z\right) - \frac{15}{4} {}_1F_1\left(\frac{7}{2}; 3; z\right) \right) \\ &= \frac{1}{2} e^z \left({}_1F_1\left(\frac{3}{2}; 2; z\right) - {}_1F'_1\left(\frac{3}{2}; 2; z\right) \right) = \frac{1}{8} e^z {}_1F_1\left(\frac{3}{2}; 3; z\right) > 0 \end{aligned}$$

Finally, property *iii* can be proved using the asymptotic expansion of ${}_1F_1(a; b; z)$ given in equation (9). To this end, rewrite

$$\begin{aligned} S_1(z; \lambda) &= \frac{1}{\sqrt{\pi} e^z} \left(\sum_{m=0}^{M-1} \frac{1}{(-z)^m} \left(\frac{3A_m}{z^{5/2}} - \frac{2B_m}{z^{3/2}} \right) + \mathcal{O}_1\left(\frac{1}{z^M}\right) \right) \\ &\quad + \frac{4}{\sqrt{\pi}} \left(\sum_{q=0}^{Q-1} \frac{z^{1/2}}{z^q} (C_q - D_q) + \mathcal{O}_2\left(\frac{1}{z^Q}\right) \right), \quad (19) \end{aligned}$$

where $z = \frac{r^2}{\lambda^2}$ and, under the assumption of sufficiently large M and Q , the magnitude of the residues $\mathcal{O}_1(1/z^M)$ and $\mathcal{O}_2(1/z^Q)$ are negligible.

In the above,

$$A_m = \frac{1}{m!} \prod_{k=0}^{m-1} \left(\frac{3}{2} + k \right) \left(\frac{5}{2} + k \right), \quad (20)$$

$$B_m = \frac{1}{m!} \prod_{k=0}^{m-1} \left(\frac{3}{2} + k \right)^2, \quad (21)$$

$$C_q = \frac{1}{q!} \prod_{k=0}^{q-1} \left(k - \frac{1}{2} \right)^2, \quad (22)$$

$$D_q = \frac{1}{q!} \prod_{k=0}^{q-1} \left(k - \frac{1}{2} \right) \left(k - \frac{3}{2} \right), \quad (23)$$

with $A_0 = B_0 = C_0 = D_0 = 1$.

Next, observe that $\frac{2B_m}{z^{3/2}}$ decreases slower than $\frac{3A_m}{z^{5/2}}$ at large z , such that $\lim_{r \rightarrow \infty} \frac{3A_m}{z^{5/2}} - \frac{2B_m}{z^{3/2}}$ is surely negative. Furthermore, $(C_q - D_q) = \prod_{k=0}^{q-1} \left(k - \frac{1}{2} \right) = -\frac{1}{2} \prod_{k=1}^{q-1} \left(k - \frac{1}{2} \right) < 0, \forall q > 0$.

Therefore, both terms in equation (20) are strictly negative and, due to the presence of e^{-z} and z^{-q} , vanishing with increasing z , thus

$$\lim_{r \rightarrow \infty} S_1(r; \lambda) = 0^-. \quad (24) \quad \square$$

Lemma 2 (Properties of $S_2(r; \lambda)$):

- i) $S_2(0; \lambda) = -3/4$
- ii) $S'_2(r; \lambda) > 0$
- iii) $\lim_{r \rightarrow \infty} S_2(r; \lambda) = 0^-$

Proof: Omitted as it follows the same steps of the proof of Lemma 1.

Proposition 1 (Convexity of $s(r; \lambda)$):

$$\exists \lambda \in \mathbb{R}^+ \mid s''(r; \lambda) > 0, \forall r. \quad (25)$$

Proof: Invoke Lemmas 1 and 2 to obtain

$$0 > S_1(r; \lambda) \geq -1, \quad (26)$$

$$0 > S_2(r; \lambda) \geq -3/4. \quad (27)$$

Next, consider equation (15). Clearly, in order for $s''(r; \lambda)$ to be negative $S_1(r; \lambda)$ and $S_2(r; \lambda)$ must be negative, such that in worst case we have (at the lower bounds)

$$\begin{aligned} s''(r; \lambda) &\geq 2 - 1.5 \frac{\sqrt{\pi} \tilde{d} r}{\lambda^3} - \sqrt{\pi} \tilde{d} \left(\frac{1}{\lambda} - \frac{2r}{\lambda^3} \right), \\ &\geq 2 - \frac{\sqrt{\pi} \tilde{d}}{\lambda} + 5 \frac{\sqrt{\pi} \tilde{d} r}{\lambda^3} \geq 2 - \frac{\sqrt{\pi} \tilde{d}}{\lambda}, \end{aligned} \quad (28)$$

where the last step results from a trivial inequality.

From the above, a lower bound on λ to ensure that $s''(r; \lambda) > 0$ is

$$\lambda \geq \frac{\sqrt{\pi} \tilde{d}}{2} \in \mathbb{R}^+. \quad (29)$$

Invoking Proposition 1, and given the data, it is found that the value of λ sufficiently large to ensure the convexity of $\langle s \rangle_{\lambda^{(1)}}(\hat{\mathbf{x}})$ is given by

$$\lambda \geq \frac{\sqrt{\pi}}{2} \max_i \{ \tilde{d}_i \}. \quad (30)$$

IV. ILLUSTRATION AND SIMULATION RESULTS

A. Illustrations and Discussion

For the sake of illustration, consider the source-localization problem applied to a network³ of $N_A = 3$ anchors (white squares) and 1 target (white ball), as illustrated in figure 1. Assume that n_i is a Gaussian random variable with the same statistics for all anchor-target links. Therefore, each term ϵ_i in equation (2) can be weighted equally, *i.e.* $w_i = 1 \forall i$ [3].

In figure 1, the contour plots of the cost-function $s(\hat{\mathbf{x}})$ obtained for both $q = 1$ (R-LS) and $q = 2$ (SR-LS) are shown. It is noticed that the location estimate $\hat{\mathbf{x}}$, obtained as the solution of the R-LS formulation, corresponds to a point closer to the true node location. The plot shows also that the objective function obtained with $q = 1$ is in general more difficult to optimize, since a larger number of local minima may appear (2 in the specific example).

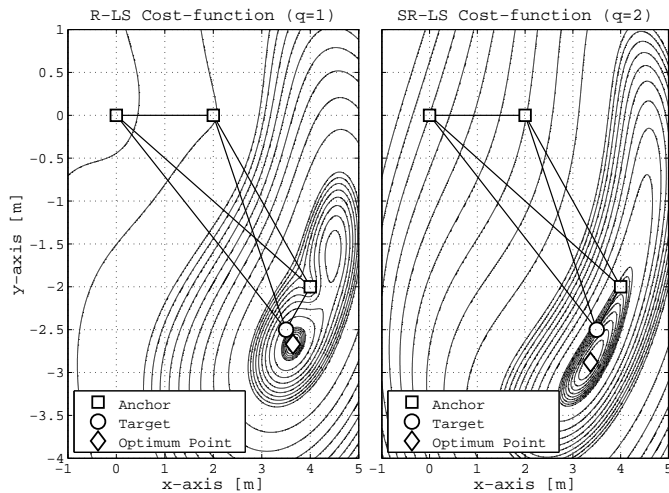


Fig. 1. Contour plot of the cost-function $s(\hat{\mathbf{x}})$ evaluated for a wireless network consisting of $N_A = 3$ anchors and 1 target.

³Coordinates: $\mathbf{a}_1 = (0, 0)$, $\mathbf{a}_2 = (2, 0)$, $\mathbf{a}_3 = (4, -2)$ and $\mathbf{x} = (3.5, -2.5)$. Noise variance: $\sigma_i^2 = 0.25$, $\forall i$. Errors: $\epsilon_1 = 0.0908$, $\epsilon_2 = 0.3613$ and $\epsilon_3 = -0.0039$.

Contour Plot of the Smoothed Function

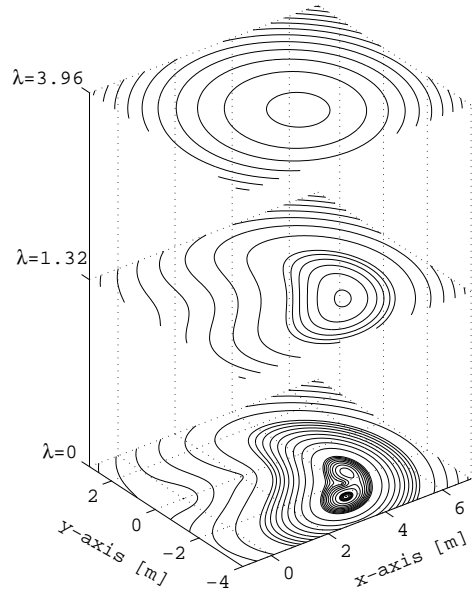


Fig. 2. Example of the smoothing effect due to the Gaussian transformation applied to the R-LS objective function related to the network example given in section II. For each level of smoothing, the contour plots of the smoothed function $\langle s \rangle_{\lambda}$ are drawn.

Considering the same example, in figure 2, instead, we show how the GDC algorithm would perform the minimization of the R-LS based objective function. Using equation (30), we compute the value of $\lambda^{(1)} = 3.96$ which, as illustrated with the contour plot at the top of figure 2, makes the smoothed function $\langle s \rangle_{\lambda^{(1)}}(\hat{\mathbf{x}})$ convex. Next, the algorithm proceeds by cooling the value of λ . For instance, taking a snapshot the smoothed function computed for $\lambda = 1.32$, it can be noticed that the minima (still 1) of $\langle s \rangle_{\lambda^{(1)}}(\hat{\mathbf{x}})$ is biased towards the global minimum of the original $s(\hat{\mathbf{x}})$. Finally, at the value of $\lambda = 0$, we observe that the smoothed-function exactly coincide with the original one.

B. Simulation Results and Comparisons

In this subsection, the performance of the proposed GDC algorithm is shown via simulations.

The typical network consists of $N_A = 3$ anchors and one target, which are deployed in a square of edge-length equals to 1 with a uniform distribution. Full connectivity is assumed and each anchor-target link is measured only once.

The first study investigates the capability of the proposed optimization to find the global optimum of the cost-function used in the R-LS formulation and we compare its performance to that one of a Newton-based non-linear LS (NLS) optimization method of similar complexity. In order to measure this performance, we evaluate over 100 set of distance measurements and several scenarios, the metric

$$\zeta = \|\hat{\mathbf{x}} - \mathbf{x}^*\|_2, \quad (31)$$

which indicates the error between the estimate $\hat{\mathbf{x}}$, obtained as the solution of a minimization technique, and the optimum point \mathbf{x}^* found from a grid-based (grid resolution $\Delta = 10^{-4}$) exhaustive search method, that in optimization theory is the equivalent of the maximum-likelihood (ML) estimator.

In figure 3, the box-plots of the statistics of ζ are shown, where the bottom-line, the middle-line and the top-line of each box indicate the 25, 50, 75 percentile (p) of the resulting ζ given a particular scenario. Thereby, the variance of the ranging error was set to 0.01.

From a qualitative analysis of the box-plot, the performance of the proposed GDC-based optimization clearly shows that the algorithm finds almost surely the optimum solution. Furthermore, the small size of the boxes indicates that the performance are very stable. The above considerations can be better understood by comparing the numerical values of 25, 50, 75 percentile, reported in table I.

The second and final study investigates the localization error performance, which is given by

$$\epsilon = \|\hat{\mathbf{x}} - \mathbf{x}\|_2. \quad (32)$$

Both the empirical cumulative distribution function (cdf) and the mean value of ϵ , respectively denoted by χ and μ , are computed. The cdf is a metric that can be used to quantify the probability that the error ϵ is below a given precision (threshold) ξ . Mathematically, it computes the probability

$$\chi = \Pr(\epsilon \leq \xi). \quad (33)$$

The mean value of ϵ , instead, gives an information about the average performance of a certain algorithm used as a source-localization estimator. This metric can be computed as

$$\mu = \frac{1}{M} \sum_{m=1}^M \epsilon^{(m)}, \quad (34)$$

where M indicates the total number of simulated networks.

In figures 4 and 5, the plots of cdf of ϵ and the mean value μ are shown for the proposed GDC algorithm, and two alternative solutions, namely, the GDC-based algorithm applied to the SR-LS problem formulation and the NLS algorithm applied to the R-LS problem. Furthermore, in the same plots the performance of a ML-equivalent algorithm obtained from a grid-based search are shown and used as benchmark. The results reveals that regardless the level of noise, which is obtained by varying σ within (0.02, 0.2), the proposed GDC-based algorithm, not only outperforms the considered alternatives, but also achieves the optimal performance given by the ML-equivalent approach.

TABLE I
STATISTICS ON THE ERROR OVER THE GLOBAL OPTIMUM ESTIMATE

n \ p	R-LS GDC ($\times 10^{-5}$)			R-LS NLS ($\times 10^{-5}$)		
	25%	50%	75%	25%	50%	75%
1	3	5	6	63	530	24519
2	2	4	5	18	77	452
3	3	4	5	13	59	715
4	3	4	5	8	38	229
5	3	4	7	365	2278	77503
6	3	4	5	29	230	1933
7	3	4	6	8	69	201
8	3	4	5	24	87	312
9	2	4	5	142	1090	68333
10	3	4	5	16	70	349
11	3	4	5	13	45	395
12	3	4	5	29	136	669

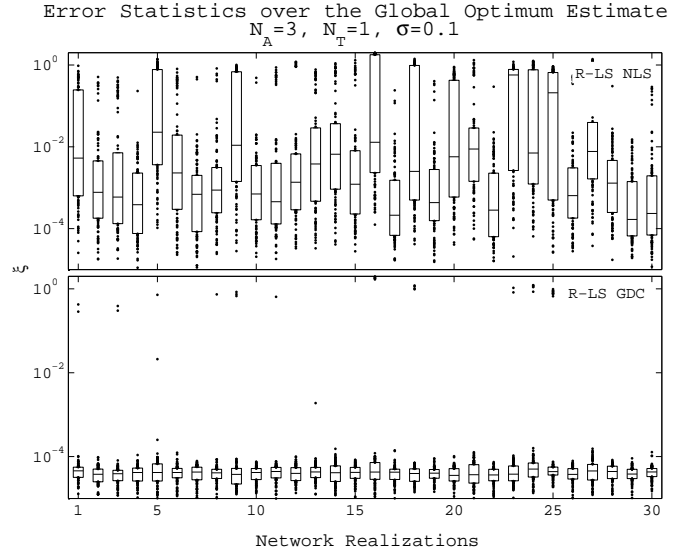


Fig. 3. Box-plot of the error statistics of ζ for the proposed GDC-based Localization Error Performance

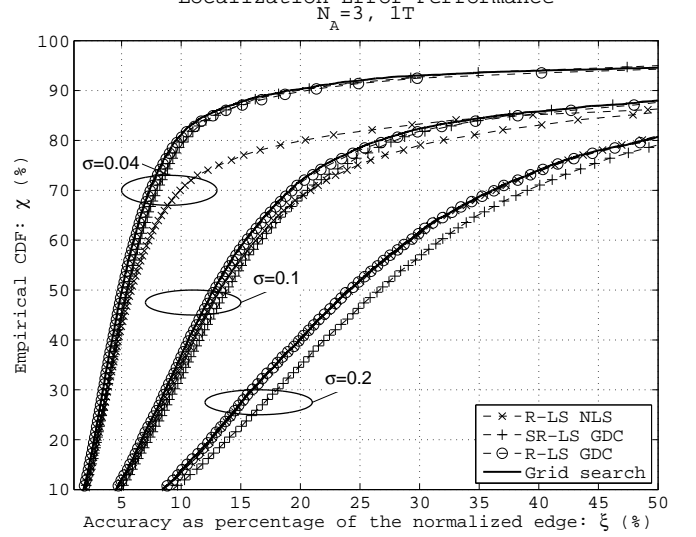


Fig. 4. Comparison of the localization error performance for different optimization algorithms: empirical cumulative distribution function

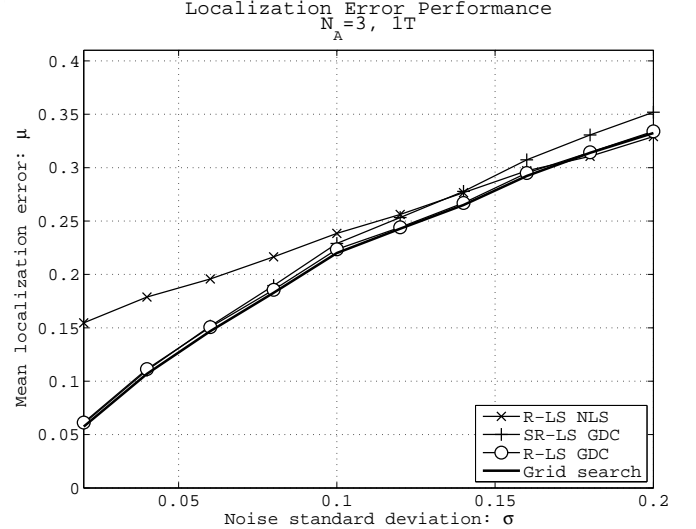


Fig. 5. Comparison of the localization error performance for different optimization algorithms: root-mean-square error.

APPENDIX

A. Derivation of $\langle s \rangle_\lambda$

Consider the analytical formula of $\langle s \rangle_\lambda$ given in equation (5), developing the integral, it can be rewritten as:

$$\langle s \rangle_\lambda(\hat{\mathbf{x}}) = \frac{1}{\pi} \sum_{i=1}^{N_A} w_i (\mathcal{I}_1 + \mathcal{I}_2 - 2\tilde{d}_i \mathcal{I}_3), \quad (35)$$

where

$$\mathcal{I}_1 = \int_{-\infty}^{+\infty} \int_{-\infty}^{+\infty} \tilde{d}_i^2 e^{u_x^2 + u_y^2} du_x du_y \quad (36)$$

$$\mathcal{I}_2 = \int_{-\infty}^{+\infty} \int_{-\infty}^{+\infty} ((\Delta_{x_i} + \lambda u_x)^2 + (\Delta_{y_i} + \lambda u_y)^2) e^{u_x^2 + u_y^2} du_x du_y \quad (37)$$

$$\mathcal{I}_3 = \int_{-\infty}^{+\infty} \int_{-\infty}^{+\infty} \sqrt{(\Delta_{x_i} + \lambda u_x)^2 + (\Delta_{y_i} + \lambda u_y)^2} e^{u_x^2 + u_y^2} du_x du_y \quad (38)$$

where the components of \mathbf{u} are explicitly written as u_x, u_y , and vector components of the difference $\mathbf{a}_i - \hat{\mathbf{x}}$ are denoted by $\Delta_{x_i} \triangleq x_{a_i} - \hat{x}_i$ and $\Delta_{y_i} \triangleq y_{a_i} - \hat{y}_i$.

Hereafter, the subscript i is omitted for notational convenience.

1) *Derivation of \mathcal{I}_1* : The integral \mathcal{I}_1 is simply equal to:

$$\mathcal{I}_1 = \pi \tilde{d}^2. \quad (39)$$

2) *Derivation of \mathcal{I}_2* : Using known properties of the Gaussian transformations [8], \mathcal{I}_2 is given by

$$\mathcal{I}_2 = \pi(\tilde{d}^2 + \lambda^2). \quad (40)$$

3) *Derivation of \mathcal{I}_3* : Using the change of variables

$$\begin{cases} \Delta_x + \lambda u_x = \rho \cos \theta, \\ \Delta_y + \lambda u_y = \rho \sin \theta. \end{cases} \quad (41)$$

\mathcal{I}_3 can be rewritten as

$$\begin{aligned} \mathcal{I}_3 &= \frac{1}{\lambda^2} \int_0^{+\infty} \int_0^{2\pi} \rho^2 e^{-\frac{1}{\lambda^2}(\rho^2 + \tilde{d}^2 - 2\rho(\Delta_x \cos \theta + \Delta_y \sin \theta))} d\rho d\theta \quad (42) \\ &= \frac{1}{\lambda^2} e^{-\frac{1}{\lambda^2}\tilde{d}^2} \int_0^{+\infty} \rho^2 e^{-\frac{1}{\lambda^2}\rho^2} d\rho \int_0^{2\pi} e^{\frac{2}{\lambda^2}\rho(\Delta_x \cos \theta + \Delta_y \sin \theta)} d\theta. \end{aligned}$$

Now, the integral on θ admits a close-form solution, that can be obtained from [17, pp. 336, eq. 3.338–4.6] by replacing $(a = 0, p = 0, q = 0, b = \frac{2\rho\Delta_x}{\lambda^2}, c = \frac{2\rho\Delta_y}{\lambda^2})$ and performing the change of variables $\phi = \theta + \pi$. Thus,

$$\mathcal{I}_3 = \pi \int_0^{+\infty} \frac{2\rho^2}{\lambda^2} e^{-\frac{1}{\lambda^2}\rho^2} e^{-\frac{1}{\lambda^2}\tilde{d}^2} I_0\left(\frac{2\rho\tilde{d}}{\lambda^2}\right) d\rho, \quad (43)$$

where $I_0(\cdot)$ is the modified Bessel function of the first kind of 0-order.

It is noticed that the remaining integral on ρ can be seen as the first moment of a Rice distribution $\mathcal{R}(r, s, \sigma^2)$ [18, pp.46-47] with $s = \tilde{d}$ and $\sigma^2 = \lambda^2/2$. Therefore, computing the first moment of $\mathcal{R}(r, s, \sigma^2)$, denoted by μ_R , and given by

$$\mu_R = \int_0^{+\infty} \frac{r^2}{\sigma^2} e^{-\frac{r^2 + s^2}{2\sigma^2}} I_0\left(\frac{rs}{\sigma^2}\right) = \lambda e^{-\frac{\tilde{d}^2}{\lambda^2}} \Gamma\left(\frac{3}{2}\right) {}_1F_1\left(\frac{3}{2}; 1; \frac{\tilde{d}^2}{\lambda^2}\right), \quad (44)$$

the integral \mathcal{I}_3 yields to

$$\mathcal{I}_3 = \pi \lambda \Gamma\left(\frac{3}{2}\right) {}_1F_1\left(\frac{3}{2}; 1; \frac{\tilde{d}^2}{\lambda^2}\right) e^{-\frac{\tilde{d}^2}{\lambda^2}}. \quad (45)$$

Given the results above, the smoothed function $\langle s \rangle_\lambda$ is given by

$$\langle s \rangle_\lambda = \sum_{i=1}^{N_A} w_i \left(\lambda^2 - 2\lambda \tilde{d}_i \Gamma\left(\frac{3}{2}\right) {}_1F_1\left(\frac{3}{2}; 1; \frac{\tilde{d}_i^2}{\lambda^2}\right) e^{-\frac{\tilde{d}_i^2}{\lambda^2}} + \tilde{d}_i^2 + \tilde{d}_i^2 \right). \quad (46)$$

Notice that in the case where $z = \frac{\tilde{d}^2}{\lambda^2} \geq 10$, by force of equation (9), the integral \mathcal{I}_3 in equation (46) simplifies to

$$\begin{aligned} \mathcal{I}_3 &\approx \pi \lambda \left(\frac{1}{4} e^{-z} z^{-\frac{3}{2}} \left(\sum_{r=0}^{M-1} \frac{(-z)^{-m}}{m!} \prod_{k=0}^{m-1} \left(\frac{3}{2} + k\right) \right) \right. \\ &\quad \left. + z^{\frac{1}{2}} \left(\sum_{m=0}^{M-1} \frac{z^{-m}}{m!} \prod_{k=0}^{m-1} \left(k - \frac{1}{2}\right) \right) \right). \quad (47) \end{aligned}$$

Using equation (9) it can be also shown that $\lim_{\lambda \rightarrow 0} \mathcal{I}_3 = 2\tilde{d}_i$.

REFERENCES

- [1] H. Liu, D. Houshang, B. Pat, and J. Liu, "Survey of wireless indoor positioning techniques and systems," *IEEE Trans. Systems, Man and Cybernetics-Part C: Applications and Reviews*, vol. 37, no. 6, pp. 1067–1080, Nov. 2007.
- [2] T. F. Cox and M. A. A. Cox, *Multidimensional Scaling*, 2nd ed. Chapman & Hall/CRC, 2000.
- [3] P. Biswas, T.-C. Liang, K.-C. Toh, T.-C. Wang, and Y. Ye, "Semidefinite programming approaches for sensor network localization with noisy distance measurements," in *IEEE Trans. Autom. Sci. Eng.*, vol. 3, October 2006, pp. 360–371.
- [4] K. W. Cheung, W.-K. Ma, and H. C. So, "Accurate approximation algorithm for toa-based maximum likelihood mobile location using semidefinite programming," in *Proc. IEEE ICASSP 2004*, vol. 5, May 17-21 2004.
- [5] A. A. Kannan, G. Mao, and B. Vucetic, "Simulated annealing based wireless sensor network localization with flip ambiguity mitigation," in *Proc. IEEE 63-rd Veh. Tech. Conf.*, vol. 2, Sept. 2006, pp. 1022–1026.
- [6] J. A. Costa, N. Patwari, and A. O. H. III, "Distributed multidimensional scaling with adaptive weighting for node localization in sensor networks," *ACM J. on Sensor Netw.*, vol. 2, no. 1, pp. 39–64, Feb. 2006.
- [7] G. Destino and G. T. F. de Abreu, "Sensor localization from WLS optimization with closed-form gradient and Hessian," in *Proc. IEEE GLOBECOM'06*, Nov. 27 - Dec. 1 2006.
- [8] J. More and Z. Wu, "Global continuation for distance geometry problems," *SIAM J. Optim.*, vol. 7, pp. 814–836, 1997.
- [9] A. Beck, P. Stoica, and J. Li, "Exact and approximate solutions for source localization problems," *IEEE Trans. Signal Processing*, vol. 56, no. 5, pp. 1770–1778, May 2008.
- [10] D. Jourdan, D. Dardari, and M. Win, "Position error bound for UWB localization in dense cluttered environments," in *Proc. IEEE ICC 2006*, vol. 8, June 2006, pp. 3705–3710.
- [11] S. Venkatesh and R. M. Buehrer, "A linear programming approach to NLOS error mitigation in sensor networks," *IPSN 2006*, pp. pp. 301–308, pril 2006.
- [12] I. Guvenc, S. Gezici, F. Watanabe, and H. Inamura, "Enhancements to linear least squares localization through reference selection and ML estimation," in *Proc. IEEE WCNC*, Mar.-Apr. 2008, pp. 284–289.
- [13] S. Boyd and L. Vandenberghe, *Convex Optimization*. Cambridge University Press, 2004.
- [14] J. Dattorro, *Convex Optimization and Euclidean Distance Geometry*. Meboo Publishing, 2005.
- [15] J. Nocedal and S. Wright, *Numerical Optimization*. Springer, 2006.
- [16] M. Abramowitz and I. A. Stegun, *Handbook of Mathematical Functions with Formulas, Graphs, and Mathematical Tables*, 10th ed. Dover Publications, 1965.
- [17] I. S. Gradshteyn and I. M. Ryzhik, *Table of Integrals, Series, and Products*, 6th ed. Academic Press, Jul. 2000.
- [18] J. G. Proakis, *Digital Communications, Fourth Edition*. New York, NY: Mc-Graw-Hill, 2000.